

# CORROSION EXPERIMENTS UNDER HUMIDITY CONDITIONS USING POLARIZATION TECHNIQUES

L. Cavalli\* and A. de Rooij

European Space Agency, European Space Technology and Research Centre,  
Product Assurance and Safety Department, Materials and Processes Division,  
P.O. Box 299, 2200 AG Noordwijk, The Netherlands

Tel: +31 71 5653716, Fax: +31 71 5654992, E-mail: ton.de.rooij@esa.int

\*Now at Alcoa Aerospace, Lausanne – Switzerland, E-mail: luana.cavalli@alcoa.com

**Abstract:** Experiments were undertaken to measure the extent of galvanic corrosion of materials combinations often used in the construction of a satellite under conditions encountered during manufacturing, testing and storage of the space hardware. A standard three-electrode technique was developed – working electrode, Pt counter electrode and Saturated Calomel Electrode (SCE) -, which were able to operate inside a humidity-controlled atmosphere. This system has given appreciable results down to 60% RH. Polarization curves have been reported measured in 0.05% NaCl, 100% RH and 70% RH. The mixed potential theory is used to combine polarization curves of different materials and to obtain mixed potential and corrosion current for the bimetallic combinations.

**Keywords:** Bimetallic Corrosion Galvanic Polarization Potentiostatic

## 1 Introduction

In the construction of a satellite, two metals may have to be placed in electrical contact with one another to avoid charge build up. Requirements are often placed on the electrical resistivity of this joint. Although this may not cause anomalies or malfunctions in the space environment, it has to be borne in mind that equipment on board the manned habitats of the International Space Station experience humidity levels up to 70% RH and also that spacecraft and equipments often have to be stored on Earth for considerable periods of time and that during storage they may inadvertently be exposed to environments where galvanic corrosion can take place. In fact, this is known to have taken place on several occasions and it is for this reason that the European Space Agency has been studying the dangers involved.

The assessment of the galvanic compatibility under atmospheric conditions between two dissimilar metals is currently based on the difference of their corrosion potentials measured in 3.5% NaCl water solution<sup>1</sup>. Simple rules were drawn up in the past to translate this difference to humidity conditions. A well-known rule was when this difference was less than 0,5 V, the combination of metals was safe for use in clean room conditions. This easy rule is still in use in many places due to its simplicity and not because it is correct. There is no close relationship between the extent of galvanic corrosion under atmospheric conditions and the difference in corrosion potential measured in salt water.

Experiments were started to measure the extent of galvanic corrosion of materials combinations often used in the construction of a satellite under conditions encountered during manufacturing, testing and storage of the space hardware.

Experiments were performed in a humidity-controlled chamber at humidity levels lower than 100%. A standard three-electrode technique was developed – working electrode, Pt counter electrode and SCE - which was able to operate inside a humidity controlled atmosphere.

The examined materials were Carbon, Titanium, Nickel, Magnesium, Stainless Steel, Aluminium and the Al alloy AA7075 (Al-Zn-Cu alloy), other materials such as silver, copper, gold, zinc and solder alloys are still under investigation.

Polarization curves will be reported measured in 0.05% NaCl, 100% RH and 70% RH and on the corrosion current derived from the mixed potential theory.

## 2 Method of investigation

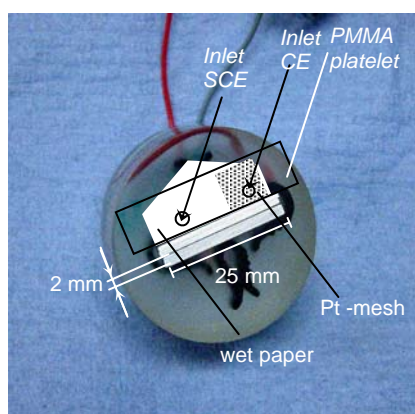
### 2.1 Potentiodynamic Polarization measurements

The electrochemical tests were performed using an electrochemical workstation IM6e from Zahner-Elektrik. The I/E experiments were performed with a polarization rate of 2mV/s, starting always at the free corrosion potential  $E_0$  and subsequently polarized anodically resp. cathodically.

The experiments under immersion conditions were performed using the classical electrode arrangement in a 0.05% NaCl solution. This solution has a conductivity of approximately 1000 $\mu$ S/cm. Experiments under a humidity-controlled atmosphere were performed in a humidity chamber controlled by an automatic humidity controller provided with a humidity sensor. An ultrasonic humidification system, rotary vent vacuum pump and a laboratory gas-drying unit provided for the desired humidity level maintenance. A fan assured equal distribution of humidity overall the chamber volume. Humidity levels could be maintained with an accuracy of +/- 2 percent points of RH%.

Each sample was shortly before testing ground with 1200 grit paper and cleaned in an ultrasonic bath with ethanol.

For electrochemical experiments under humidity conditions, specimens required some additional preparations: A previous hydrophilisation of the surface was necessary to assure an equally thick electrolyte film over the sample. This was achieved by means of a plasma treatment on air leak during approximately 1 minute using a Plasmod of Tegal Corporation. Spreading 75 $\mu$ l of a 0.05% NaCl solution on the sample surface and leaving it to dry it out activated the surface; this corresponds to a 60 $\mu$ m water layer with a conductivity of 1000 $\mu$ S/cm. The concentration of this activation solution was found to be optimal because the crystallization during drying out was very fine; bigger crystals are too hygroscopic and form drops on the surface already at humidity levels of 80% altering the experiment.



After activation, a wet paper strip - saturated with the same solution - was placed along the working electrode surface leaving a small gap of approximately 0.5 mm. This ensures high enough conductivity up to very close to the sample without affecting the water layer formed on the working electrode at the tested humidity level. To hinder the paper from drying, a transparent Plexiglas (PMMA) covering platelet was positioned over it.

**Fig. 1.** Sample for measuring single or bimetallic corrosion properties. CE: Counter Electrode; SCE: Saturated Calomel Electrode.

A Pt electrode was used as counter electrode. In order to achieve a larger counter electrode surface area in contact with the electrolyte, a Pt mesh was positioned between the Pt-tip and the wet paper strip. A Saturated Calomel Electrode (SCE) was used as reference. A Pasteur pipette filled with KCl saturated agar-agar gel acted as salt-bridge connection between the SCE and the sample surface. To avoid excessive leakage, a minuscule piece of Silly Putty was put at the pipette ending as a plug.

### 2.2 Electrochemical Impedance Spectroscopy (EIS)

The experimental setup for Impedance Spectroscopy measurements was the same as for the potentiodynamic polarization experiments for both in immersion and in the humidity chamber with an excitation amplitude of 10 mV around the corrosion potential in the frequency range from 10<sup>5</sup> Hz down to 2 · 10<sup>-2</sup> Hz.

### 2.3 Samples

The materials to be investigated were mostly delivered in 2mm thick plates, which were then cut in pieces of 25x10 mm. The wires for electrical connection were connected using soldering or - for non-solderable materials - using conductive silver glue. Couples of different materials were then potted in Caldofix resin but kept separated by an electric insulating 25µm thick mica foil. After curing, the samples were mechanically ground with 1200 grit paper in order to expose the 25x2mm edges to the desired atmosphere.

**Table I:** Composition information about the tested materials. GF: Goodfellow Cambridge Limited, Huntingdon, UK, ARM: Advent Research Material Limited, Eynsham-Oxford, UK.

	Symbol	Purity [%]	Composition	Thickness [mm]	Supplier
<b>Carbon</b>	C	99.5		2.5	GF
<b>Titanium</b>	Ti	99.6+		2.0	GF
<b>Nickel</b>	Ni	99.0+		2.0	GF
<b>AA 7075 (Al-Zn-Mg-Cu)</b>		-	Al 90/5.6Zn	2.0	Internal stock
<b>Platinum wire</b>	Pt	99.95		∅ 0.5	ARM
<b>AISI 316</b>	SS	-	Fe69/Cr18/Ni10/Mo3	1.0	GF
<b>Magnesium</b>	Mg	99.9		2.0	GF
<b>Muscovite Mica</b>		-	Potassium Aluminosilicate	0.025	GF

## 3 Results and discussion

### 3.1 Electrochemical Impedance Spectroscopy measurements

In practice the impedance plots are correlated with one or more equivalent circuits. The lower frequency region of the spectra reflects the electrochemical processes close to the electrode surface. The impedance effects at these frequencies include charge transfer resistance, a blocking capacitance and possibly a diffusion impedance. At high frequencies the spectra reflects the resistance between the working electrode and reference electrode. This Ohmic resistance is a complex matter for the chosen configuration, as it consists of the solution resistance of the gap distance and is also a function of the solution resistance of the electrolyte layer on the working electrode surface.

The solution resistances were estimated from fitting the impedance data to the proposed equivalent circuits illustrated in Fig. 5. The 0.5 mm gap and the conductivity of the electrolyte near the reference electrode of 1000 µS/cm results in a solution resistance as given in table II

To estimate the effect of the uneven current distribution due to the high resistance of the thin electrolyte layer, the measurement configuration was changed to a symmetrical electrode arrangement where the reference and counter electrode were positioned along both sides of the working electrode. A second experiment used a much thinner working electrode. Instead of 2mm, a working electrode 0.24 mm was used. Both experiments were conducted using pure aluminium as working electrode and with the 0.05% NaCl, 100% RH and 70% RH test environments. Within the error of results these measurements revealed not significant difference compared to the standard measurements.

**Table II:** Ohmic resistance over gap between working electrode and reference electrode

	70% RH	100% RH	0.05% NaCl
<b>Rs</b>	1500	700	80

It is also reported that the equivalent circuit of this type of configuration (metal-thin electrolyte) should be presented by a so-called transmission line circuit (TML)<sup>2</sup>. TML behaviour is indicated by a phased shift going no further than 45° in a Bode-phase plot and a linear part with a slope of

$-\frac{1}{2}$  on a Bode-impedance plot. We see this effect in Figs. 2 and 3 for the tests performed at 100% RH and in  $18\mu\text{S}/\text{cm}$  water. Tests performed at 70% RH do not show TML behaviour. This is probably due to the drying out of the filter paper supporting the reference electrode and counter electrode during the long measuring times required at the lower measuring frequencies.

Calculating the effect of non-uniform current distribution using the model of Nishikata<sup>2</sup> a minimal effect is expected. The limited effect is attributed to the increasing conductivity of the thin electrolyte layer during drying out of the original  $60\mu\text{m}$ - $1000\mu\text{S}/\text{cm}$  water layer, thus increasing the conductivity of the electrolyte layer, which results in reducing the effect of the non-uniform current distribution.

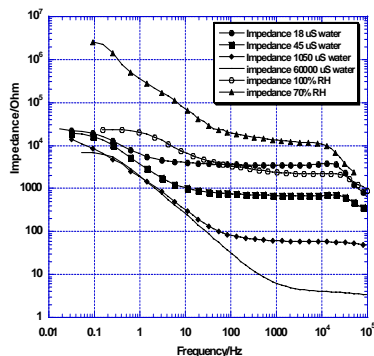


**Fig. 2.** Bode-impedance Plot comparison of Al with the same electrode configuration

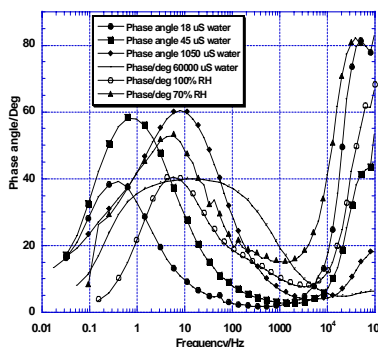


**Fig. 3.** Bode-phase Plot comparison of Al with the same electrode configuration.

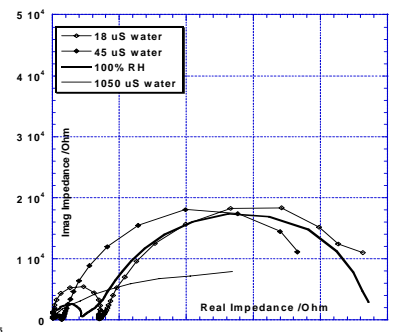


**Fig. 4.** Nyquist Plot comparison of Al with the same electrode configuration.

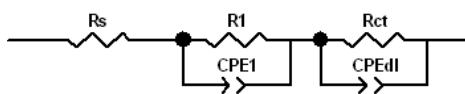


**Fig. 5.** The equivalent circuit used to fit the data for the Al electrode given in Figs. 2-4.  
 $R_s$ =Ohmic resistance over gap,  $R_{ct}$ =charge transfer resistance,  $CPE_{dl}$ = interfacial aqueous double layer capacitance

### 3.2 Potentiodynamic Polarization measurements

The solution resistance values from Table II are used to calculate the voltage drop. This correction is applied to the polarization curves displayed in Figs. 6 to 9. The correction is minimal while the currents are in the order of  $10^{-5}$  to  $10^{-7}$  A/m<sup>2</sup>.

Figs. 6-9 show average polarization curves for each of the four reported materials at 70% RH, 100% RH and their comparison with polarization curves obtained in a 0.05% NaCl solution using standard procedures. Additional materials such as Copper, Zinc and Tin-Lead were measured and included in the analysis but not displayed in the polarization graphs. The polarization curves in Figs. 6 to 9 are averages of several measurements. At each conductivity level at least three complete polarization curves are measured. The error bars in the plots depict the spread of the measured currents at the applied potential. The corrosion current is diminishing with decreasing humidity. The oxygen depolarization process becomes more and more effective with thinning of the moisture layers, because of the increased oxygen transport through these thin layers<sup>3</sup>. This process cannot go on forever towards extremely thin absorbed moisture films encountered below 100% RH. Hindering of the cathodic depolarization can occur due to insufficient water present under these conditions. The anodic process will also be reduced as a result of the diminishing moisture layer, the result being the appearance of anodic passivity. The passive state is strongly enhanced by the increased access of oxygen to the surface.

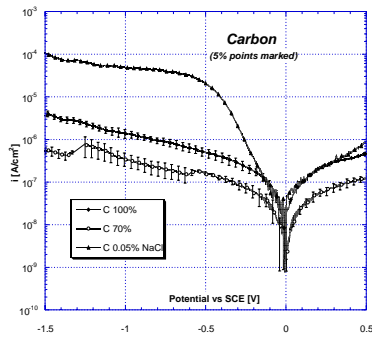


**Fig. 6.** Average polarization curves with standard deviation for Carbon.

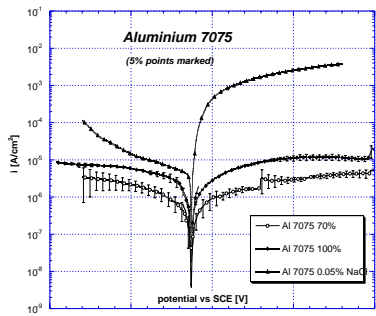


**Fig. 7.** Average polarization curves with standard deviation for AA7075.

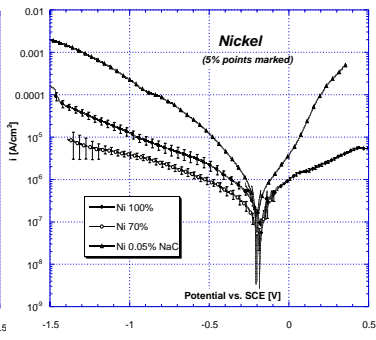


**Fig. 8.** Average polarization curves with standard deviation for Nickel.

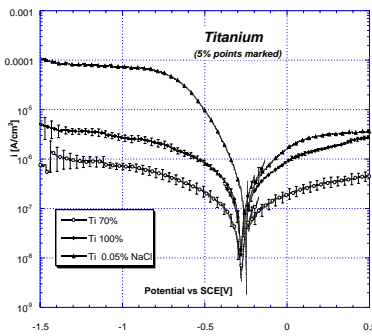


**Fig. 9.** Average polarization curves with standard deviation for Titanium.

In all investigated metals the same trend can be observed. The corrosion current  $I_0$  (calculated from the polarization curves) is decreasing with decreasing humidity. This is confirmed by the increase of the polarization resistance  $R_p$  as determined in the Bode-impedance plot in Fig. 2 at the low frequencies. The corrosion current  $I_0$  depends on the position in the galvanic series. In general the nobler the material the lower is the corrosion current. This is confirmed by the calculated values in table III. Tafel slopes obtained from these measurements are unreliable, while each curve displayed in the figures is the average of several individual ones.

**Table III.** Corrosion currents  $i_{\text{corr}}$  for the investigated couples using the mixed potential theory

$i$ [ $\mu\text{A}/\text{cm}^2$ ]	$i_{\text{mix}}$ 0.05% NaCl	$i_{\text{mix}}$ 100%RH	$i_{\text{mix}}$ 70%RH
Al 7075-Ti	27	1.20	0.30
Al 7075-Ni	27	2.40	0.92
Al 7075-C	32	0.63	0.16
Al 7075-Mg	130	6	1
Al 7075-SS	35	3.4	0.54
Ti-C	0.32	0.19	0.06
Ti-Ni	0.21	0.20	0.06
Ti-SS	0.42	0.35	0.097
Ti-Mg	87	3.6	0.89
Mg-Ni	390	9	1.2
Mg-SS	200	5.9	0.89
Mg-C	73	2.9	0.5
SS-Ni	0.38	0.19	0.097
SS-C	0.1	0.11	0.04
C-Ni	0.25	0.14	0.05
Mg *	40	0.8	0.3
Al 7075 *	5	1.5	0.4
Ti *	0.9	0.1	0.07
Ni *	2	0.5	0.2
AISI316*	1	0.6	0.25
C *	0.1	0.09	0.02

\* These values are not mixed corrosion currents  $i_{\text{mix}}$  but the  $i_{\text{corr}}$  of the single members of the couples calculated from the polarization curves.

The mixed corrosion current and mixed potential for a specific materials combination can be obtained from measuring the couple explicitly. Great reduction in measurement effort is achieved using the mixed potential theory<sup>4</sup>. Comparison of data at 100% RH given in Fig. 10 between direct measurements on the Al-Ti combination and using the mixed potential theory when combining the individual Al and Ti results shows that both methods reveal very similar results. This method is used for obtaining the results shown in table III. The observation that the corrosion current is changing in one direction when lowering the humidity is also true for the mixed potential. As illustrated in Fig. 11 the combination of Aluminium vs. Nickel and using the mixed potential theory shows that the mixed potential becomes more nobler with decreasing humidity. In all cases the mixed potential of metal combinations is close to the corrosion potential of the anodic member. The lower corrosion current of the cathodic member (nobler) of the combination and the shape of the cathodic curve of the nobler metal following the hindering of the cathodic depolarization as explained in the beginning of this section, explains why this type of corrosion under the circumstances given is cathodically controlled. This means with material

combinations having the same cathodic member, the mixed properties can be estimated from the relative position of the corrosion potential of the anode in relation to the cathode.

#### 4 Conclusions

A relatively easy classical three electrode configuration for polarization experiments in not immersed environments has been successfully developed and subsequently tested by performing potentiodynamic polarization experiments on Al, Ti, Ni, SS, Mg and Carbon in a humidity chamber at different humidity levels. The system has given appreciable results down to 60% RH and the adopted electrode disposition gave comparable results to tests performed with the standard arrangement advised by the American Society for Testing and Materials, which is however only possible to use in immersion.

The mixed potential theory could be confirmed as applicable also in humidity-controlled atmospheres. The corrosion behaviour under atmosphere conditions was found not to be in line with the one obtained in aqueous conditions, therefore no experiments in immersion should be taken to explain corrosion behaviour in atmospheric conditions.

The developed method allows the acquisition of quantitative information directly in the environment of interest and considerably reduces the amount of experiments necessary to define the mixed corrosion properties. Once a polarization curve for a material is determined, it is possible to combine it with every other material without any need of producing a specific bimetallic sample. For qualitative prediction of galvanic corrosion behaviour, corrosion rates can even be estimated by assuming that the polarization curve must be included between already measured curves of two other similar materials sitting at the left and at the right side in the galvanic series.

#### 5 Acknowledgements

The authors would like to thank all staff of the laboratories of the Materials, Mechanics and Processing Section of ESTEC – the European Space Research and Technology Centre, the European Space Agency.

#### 6 References

- [1] ECSS-Q-70-71A, *Data for selection of space materials and processes*. 2004, European Cooperation on Space Standardization.
- [2] Nishikata, A., Y. Ichihara, and T. Tsuru, *An Application of electrochemical Impedance spectroscopy to Atmospheric Corrosion Study*. Corrosion Science, 1995. **37**(6): p. 897-911.
- [3] Tomashov, N.D., *Theory of Corrosion and Protection of Metals*. 1st ed. The Science of Corrosion, ed. I.G. Translated and edited by B.H. Tytell, H. S. Preiser. 1966, New York: The MacMillan Company.
- [4] Wagner, C., W., *Über die Deutung von Korrosionsvorgängen durch Überlagerung von Electrochemischen Teilvorgängen und über die Potentialbildung an Mischelektroden*. Zeitschrift für Elektrochemie und angewandte Physikalische Chemie, 1938. **44**(7): p. 391-454.

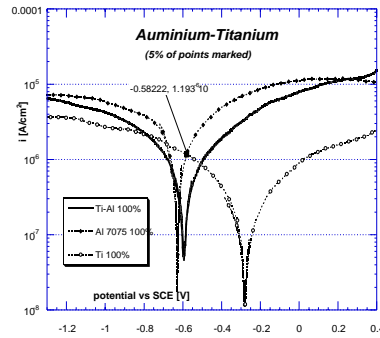


**Fig. 10.** Mixed potential theory compared with the direct experiment of the couple Al-Ti at 100% RH.

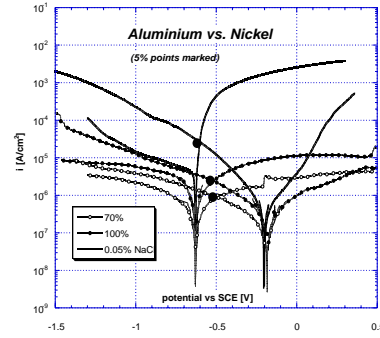


**Fig. 11.** Example of mixed potential theory applied to potentiodynamic curves of Al and Ni. The mixed potential becomes nobler with decreasing humidity.